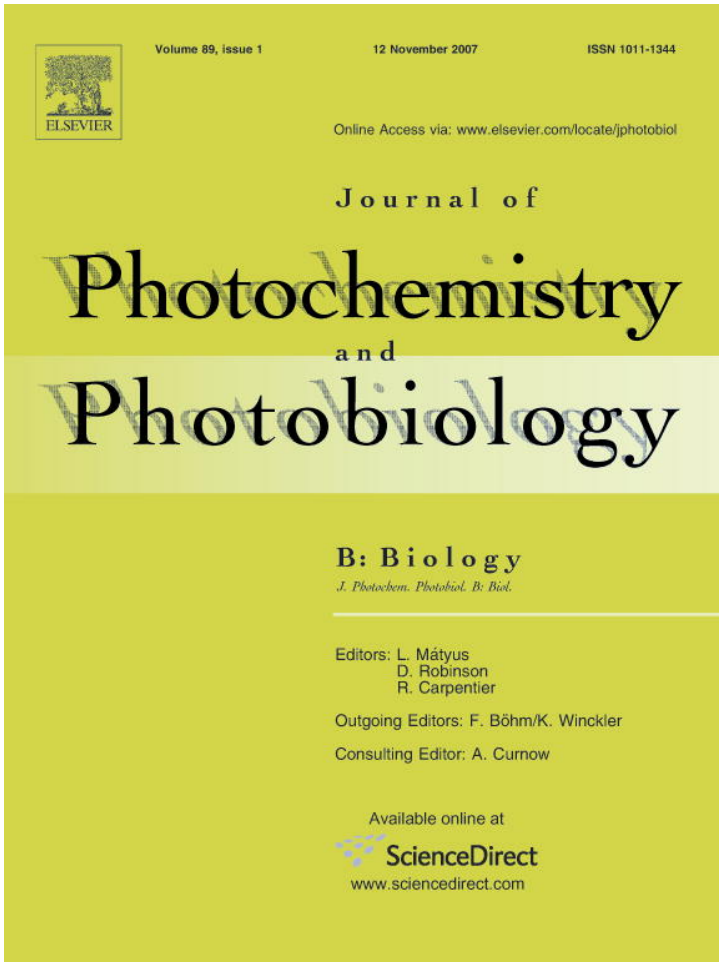

Available online at www.sciencedirect.com
ScienceDirect
Journal of Photochemistry and Photobiology B: Biology 89 (2007) 56–62
Journal of Photochemistry and Photobiology B:Biology
www.elsevier.com/locate/jphotobiol

Spectroscopic probing of *ortho*-nitrophenol localization in phospholipid bilayers

Julieta M. Sánchez, Anahí del V. Turina, María A. Perillo *

Biofisica-Química, Depto. de Química, Facultad de Ciencias Exactas, Físicas y Naturales, Universidad Nacional de Córdoba, Av. Velez Sarsfield 1611, X 5016GCA Córdoba, Argentina

Received 2 May 2007; received in revised form 21 August 2007; accepted 23 August 2007
Available online 6 September 2007

Abstract

In the present study we estimated the localization of *ortho*-nitrophenol (ONP) within model membranes through its efficiency to quench and to modify the anisotropy of DPH and TMA-DPH fluorescence. These fluorescent probes are known to sense the hydrocarbon core and the polar head group region of membranes, respectively. TMA-DPH fluorescence in MLVs was more efficiently quenched than DPH ($K_{q,\text{TMA-DPH}} = 2.36$ and $K_{q,\text{DPH}} = 1.07$ mM ns^{-1}). Moreover, these results demonstrated the interfacial localization of ONP and may contribute to understand membrane-mediated mechanisms of ONP-induced toxicity and the behavior of ONP as a product of several enzymatic reactions occurring in the presence of lipid–water interfaces.

Keywords: *Ortho*-nitrophenol localization; Phospholipid vesicle; DPH, TMA-DPH; Fluorescence quenching

1. Introduction

Nitrophenols are a group of relative hydrophobic weak acids of a considerable environmental concern. These compounds are used as intermediates in the synthesis of pesticides and dyes or are directly applied as herbicides and insecticides. They also act as uncoupling agents in oxidative phosphorylation and are known to affect cell metabolism at concentrations lower than 10 μM, [1]. The sorption behavior and the microbial uptake and metabolism of nitrophenols highlights the importance of the concepts related with non-aqueous phase/water transfer processes of non-polar organic compounds in natural systems, [2]. The bio-availability of such compounds to the target is an important consideration in the rational interpretation of their action mechanisms. They have to pass through various cellular barriers before eliciting an effect. The hydrophobicity and aromaticity of nitrophenols allows the prediction of their action at the level of the membrane and membrane-embedded proteins [3,4].

A direct relationship can be found between the amount of a particular partitioned compound and its effect on the structural integrity and functional properties of membranes. However, the type of hydrophobic interaction and the depth within the membrane where the lipophilic compound resides will determine the extent to which the membrane will be expanded [5,6], the correlation between the extent of expansion and the molar volume of the compound [7] as well as the extraction of phospholipids through budding transformation [8]. The latter depends on the interplay of spontaneous curvature, bending rigidity and line tension within a fluid membrane domain that may be induced by drug accumulation [5–8].

One of the nitrophenols, the nitro substituted at the ortho position to the phenolic group (*ortho*-nitrophenol, ONP), is one of the hydrolysis products generally used as artificial substrates in enzyme kinetic studies, e.g., β-galactosidases [9,10]. The rates of these reactions are frequently determined by measurements of the absorbance of the

* Corresponding author. Tel.: +54 351 4344983; fax: +54 351 4334139.
E-mail address: mperillo@efn.uncor.edu (M.A. Perillo).

1011-1344/$ - see front matter © 2007 Elsevier B.V. All rights reserved.
doi:10.1016/j.jphotobiol.2007.08.004

formed product. If the membrane–water partition coefficient of the product is non-zero, as may be expected for ONP ($P_{\text{octanol–water, ONP}} > 0$) [1,11], the magnitude determined for the reaction rate may be affected in the presence of membrane–water interfaces. This is due to the difference between the extinction coefficient of the membrane partitioned ONP (ε_m) and the corresponding value in water (ε_w), leading to $\varepsilon_m - \varepsilon_w \neq 0$ [12]. Moreover, ε_m, being sensitive to the environment polarity, will depend on the localization of ONP within the membrane.

The present study was aimed at estimating the localization of ONP within model membranes to contribute to the understanding of the membrane-mediated mechanism of ONP induced toxicity as well as the enzyme kinetics in heterogeneous systems. The approach used was the evaluation of the quenching efficiency of ONP against two fluorescent probes, diphenylhexatriene (DPH), known to be located within the hydrocarbon chain region of the membrane core and a parent compound, trimethyl ammonium diphenylhexatriene (TMA-DPH), which stabilizes its DPH moiety at the polar head group region of bilayers [13]. Anisotropy measurements helped to evidence that ONP affects the molecular organization of the bilayer.

2. Materials and methods

2.1. Materials and experimental procedures

All reagents and solvents used were of analytical grade. *ortho*-nitrophenol (ONP) obtained from ICN Pharmaceuticals (Costa Mesa, CA), DPH and TMA-DPH from Sigma Chem. Co (St. Louis, MO) and lipids (egg–phosphatidylcholine, EPC, and dipalmitoyl-phosphatidylcholine, dpPC) purchased from Avanti Polar Lipids (Alabaster, Alabama) were used without further purification.

MLVs were prepared as described elsewhere [14] [from a dry film obtained by evaporating, under a stream of N_2, the $HCCl_3$ from a solution of pure lipid, EPC or dpPC (the later was used only in anisotropy experiments). The lipid was suspended in water at a final concentration of 1.3 mM, by repeating six consecutive cycles of heating at 21 °C (EPC) or 50 °C (dpPC) for 2 min plus vortexing for 1 min (note: liquid crystalline–gel phase transitions are -5.8 ± 6.5 °C and 41.6 ± 0.8 °C for EPC and dpPC, respectively [15]). Under these conditions, phospholipids self-aggregated in multilamellar vesicles [15]. Emission spectra of DPH or TMA-DPH (6 μM) in the presence or in the absence of MLVs (lipid concentration 0.66 mM) and ONP (0–0.8 mM or up to 1.6 mM in anisotropy experiments) were recorded at 426 nm (exciting at 356 nm) by using an L-format Fluoromax Spex-3 Jovin Yvon (Horiba, NJ, USA) spectrofluorimeter, equipped with a thermostated cell holder, a Xenon arc lamp, a photomultiplier tube as a signal detector and a photon counting module. Excitation and emission slits width were set at 2 nm. At the EPC concentration used the fluorescence intensities of DPH and TMA-DPH at 426 nm (FI_{426}) were within a linear range. Background and scatter intensities were measured on a blank sample with ONP added and subtracted from the readings of the other samples, at the corresponding ONP concentration. This also allowed the correction for ONP-induced inner filter effects. The possibility that ONP could promote a decrease in the size of MLVs, was discarded because the light scattering estimated from the absorbance intensity at 650 nm exerted by a fixed concentration of lipids was independent of ONP concentration.

2.2. Data analysis

2.2.1. Static–dynamic quenching model

Experimental values were analyzed under a modified Stern–Volmer equation (Eq. (1)) that took into account the fluorescence decrease induced by the collision of the quencher with the fluorophore in the excited state (dynamic quenching) and, simultaneously, the formation of a non-fluorescent complex between the quencher and the fluorophore in a non-excited state (static quenching) [16]:

$$F_0/F = 1 + (K_D + K_S)[Q] + K_D K_S [Q]^2 \quad (1)$$

where F_0 and F are the fluorescence intensities (FI) in the absence and in the presence of a quencher concentration $[Q]$, K_D and K_S are the Stern–Volmer constants for the dynamic and the static quenching, respectively, and they can be estimated from a plot of F_0/F vs $[Q]$.

2.2.2. Sphere of action model

The second model applied (Eq. (2)) considered only dynamic quenching with F_0/F values exponentially dependent on $[Q]$ and a sample volume named the sphere of action (v) where the probability of quenching would be the unity:

$$F_0/F = [1 + K_{SV} \cdot [Q]] \cdot e^{\frac{[Q] \cdot v \cdot N}{1000}} \quad (2)$$

Here, N is the Avogadro's number and F_0, F, $[Q]$ and K_{SV} are defined as above. In turn, K_{SV} depends on the bimolecular quenching constant (K_q) and the fluorescence life time (τ_0) of the probe (DPH and TMA-DPH) in the absence of quencher (ONP) as shown in

$$K_{SV} = K_q \cdot \tau_0 \quad (3)$$

2.3. Fluorescence anisotropy

Steady-state fluorescence anisotropy (A) was calculated according to

$$A = \frac{VV - VH \cdot G}{VV + 2 \cdot VH \cdot G}, \quad G = \frac{HV}{HH} \quad (4)$$

where VV, HH, VH and HV are the values of different measurements of fluorescence intensity at $\lambda_{em} = 430$ nm ($\lambda_{ex} = 356$ nm) taken with both polarizer filters oriented parallel (with vertical (VV) and horizontal (HH) orientations) or perpendicular (with excitation polarizer vertical

and emission polarizer horizontal (VH) or *vice-versa* (HV)) one with respect to the other. G is a correction factor for differences in the detection system sensitivity for vertically and horizontally polarized light [16].

2.4. Statistical calculations

The least squares method was applied to fit functions through a non-linear regression analysis. Student's t -test was applied to compare individual averages. The propagation error method was used to evaluate the error associated to calculate variables from other ones determined experimentally [17].

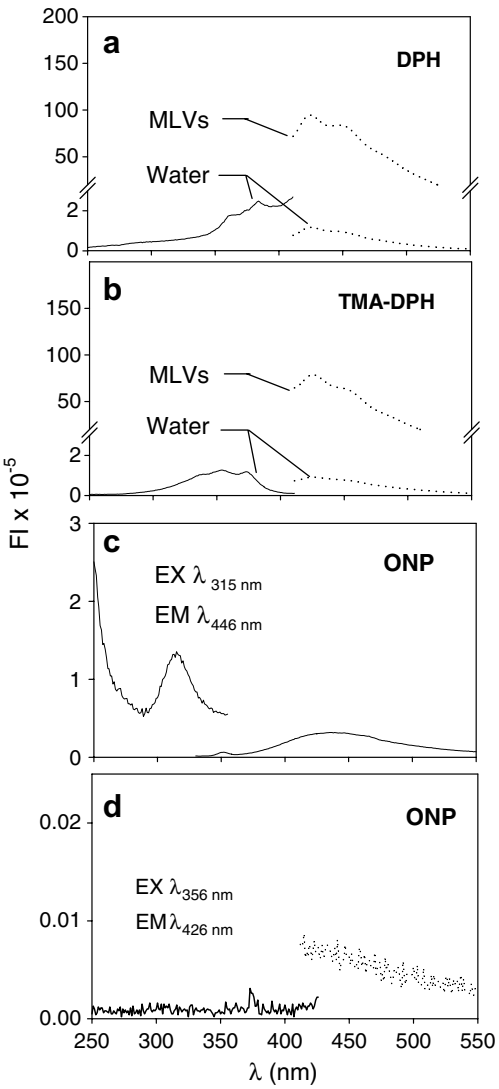

Fig. 1. Excitation and fluorescence emission spectra. DPH (a), TMA-DPH (b) and ONP (d) excitation spectra were recorded at a constant $\lambda_{em} = 426$ and the emission spectra were obtained at a constant $\lambda_{ex} = 356$. In (c) the excitation and emission spectra of ONP were recorded at $\lambda_{ex} = 315$ and $\lambda_{em} = 446$. Full lines and dotted lines indicate excitation and emission spectra, respectively.

3. Results

3.1. Experimental conditions for fluorescence studies

Fig. 1 shows excitation and emission spectra of DPH (Fig. 1a) and TMA-DPH (Fig. 1b). Their fluorescence intensity (FI) increased in the presence of MLVs with respect to water due to their partitioning towards the lipid phase ($P_{m/w,DPH} = 1.3 \times 10^6$ and, $P_{m/w,TMA\text{-}DPH} = 2.4 \times 10^5$) [18] and the increase in their quantum efficiency. ONP also exhibited an emission spectrum when excited at 315 nm (Fig. 1c) but, at the excitation wavelength of DPH, the emission of ONP was negligible (Fig. 1d), suggesting that it would not interfere with probes spectra.

3.2. Fluorescence quenching of DPH and TMA-DPH induced by ONP

The FI elicited by the experimental samples containing DPH and TMA-DPH decreased as a function of ONP concentration (Fig. 2). For the Stern–Volmer analysis the corrected FI values of DPH and TMA-DPH were used.

3.3. Stern–Volmer analysis

The ratio F_0/F for DPH and TMA-DPH recorded as a function of ONP in the presence or in the absence of MLVs showed a positive deviation from linearity (Fig. 3). Hence, two models that might explain the exponential behavior of the quenching were tested [16]: (a) static plus dynamic quenching model which considers that both types of quenching are occurring simultaneously (Eq. (1)) and (b) the sphere of action model which considers that within a particular volume (v) of the solution the probability of quenching is unity (Eq. (2)). The later model fitted better our experimental results (Fig. 3a and b) than the former (Fig. 3c and d). For these reason we used Eq. (2) in analyzing our data and the parameters determined through the non-linear regression analysis are shown in Table 1. The values of "v" indicated that the probability of collisions between DPH and ONP in the aqueous phase was higher than in the presence of MLVs and also than the encounters between TMA-DPH and ONP in both experimental conditions assayed. This is also reflected by the radii of the sphere of action r. This result is also supported by the fact that the ONP-induced quenching of DPH in solution had the highest K_{SV} and exhibited the highest sensitivity (could be achieved at the lowest ONP concentration). $K_{SV,DPH}$ suffered a 45% reduction upon DPH partitioning within MLVs while in the case of TMA-DPH, $K_{SV,TMA\text{-}DPH}$ was only 3.8% lower in MLVs than in solution.

However, in view of the differences between the life times of DPH and TMA-DPH both in solution [19] and within the lipidic environment [20,21], the concentration of ONP required to quench a 50% of fluorescence, calculated as $1/K_{SV}$, would not reflect properly the intrinsic efficiency of the quenching phenomena in each condition. So,

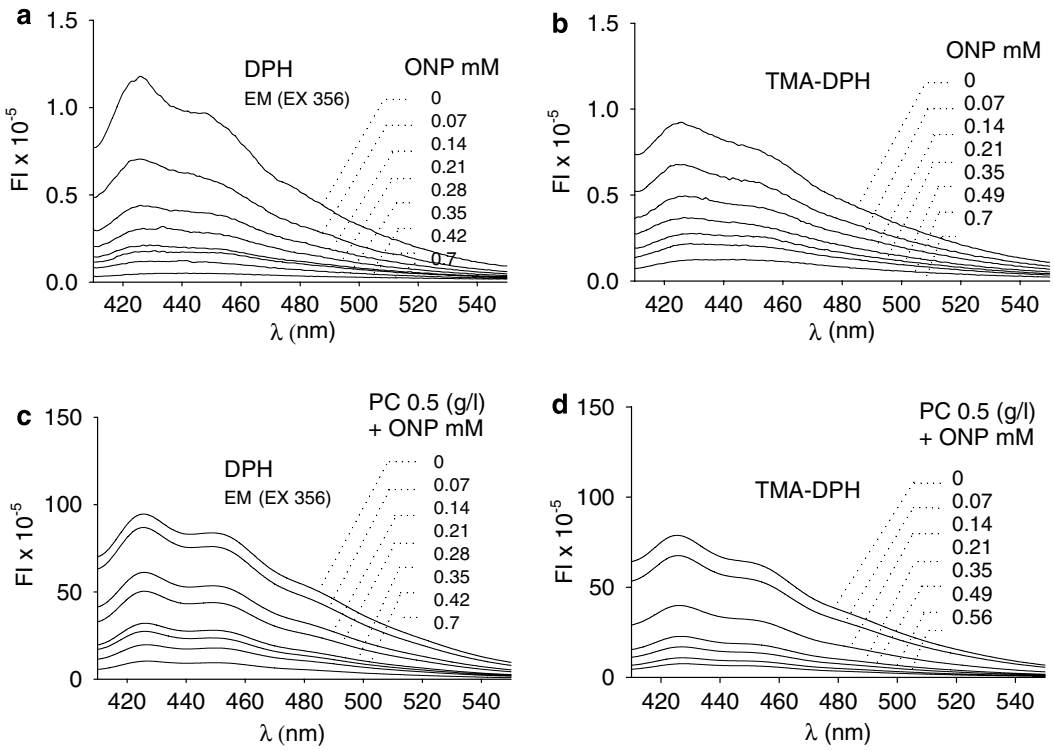

Fig. 2. Effect of ONP on the spectral behavior of DPH and TMA-DPH in the absence or in the presence of EPC-MLVs. Emission spectra of DPH (a and c) and TMA–DPH (b and d) in aqueous medium (upper panels) and in the presence of MLVs (lower panels). All spectra were registered at $\lambda_{ex} = 356$ nm. ONP concentration varied between 0 and 0.7 mM, from top to bottom.

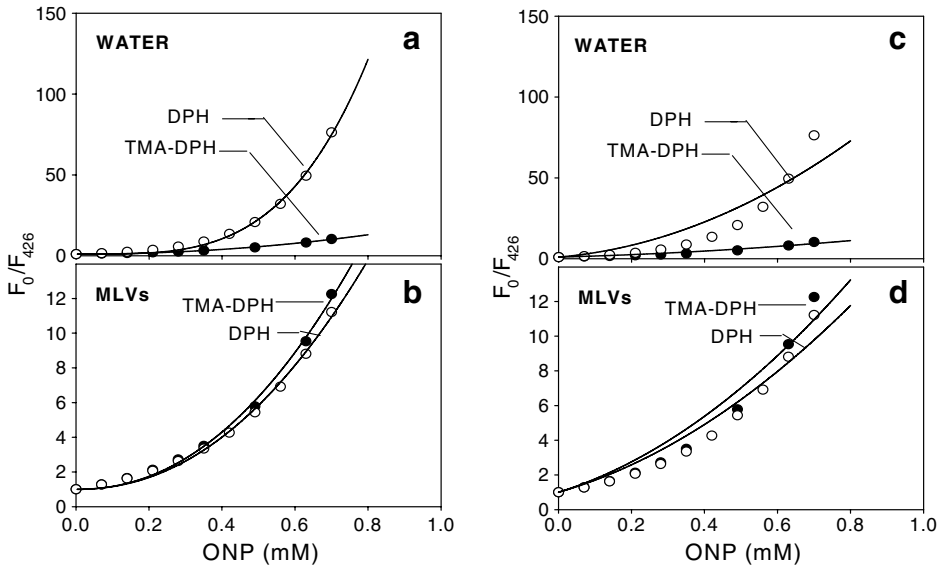

Fig. 3. Stern–Volmer plots for the ONP-induced quenching of DPH and TMA-DPH fluorescence in water or in the presence of MLVs. The ratio F_0/F was calculated from the corrected FI data (see Section 2.1). Lines in panels (a) and (b) represent the fitting to the sphere of action model (Eq. (2)) and lines in panels (c) and (d) represent the fitting to the static plus dynamic quenching model (Eq. (1)).

comparisons should be done on the basis of K_q (Eq. (3)). From this point of view, the ONP-induced quenching of both DPH and TMA-DPH were significantly greater in water than in the presence of MLVs. The result $K_{q,DPH,water} > K_{q,DPH,MLVs}$ indicated that the accessibility of ONP to DPH, in MLVs, was significantly impaired by the internalization of DPH within the membrane core. On the contrary, in the presence of membranes, the ONP-induced quenching of TMA-DPH was higher than that of DPH ($K_{q,TMA\text{-}DPH,MLVs} > K_{q,DPH,MLVs}$). Taken together these results supported the idea of ONP localization at the outer membrane region. The higher values of

Table 1
ONP-induced quenching of DPH and TMA-DPH fluorescence (Stern–Volmer analysis according to the sphere of action model)

Sample	ONP	K_{SV} ($mM^{-1} \cdot 10^{-7}$)	$[Q]_{50}$ (mM)	τ_0 (ns)	K_q^c ($mM^{-1}\ ns^{-1} \cdot 10^{-7}$)	v (cm^3/molecule)	r (Å)
Water							
DPH	+	$14.37 \pm 0.01^{\#}$	0.07	6.77^a	2.12	1.028×10^{-20}	13.49
TMA-DPH	+	$8.37 \pm 0.008^{*}$	0.12	$<1.5^a$	5.58	5.548×10^{-21}	10.98
MLVs							
DPH	+	$8.597 \pm 0.007^{\#\S}$	0.116	8^b	1.07	5.73×10^{-21}	11.10
TMA-DPH	+	$8.05 \pm 0.0067^{*\S}$	0.124	3.4^b	2.36	5.98×10^{-21}	11.26

Experimental data shown in Fig. 3a and b were fitted to Eq. (2). Values correspond to the mean ± s.e.m (non-linear regression analysis by the least squares method). #, ∗ and §: statistically different between one another with $p \ll 0.0001$. Taken from [a][19], [b][20,21]; [c]calculated from Eq. (3) [16].

$K_{q,TMA\text{-}DPH,water}$ with respect to $K_{q,DPH,water}$ as well as $K_{q,TMA\text{-}DPH,MLVs}$ may be related with the interaction of the zwitterionic ONP with the positively charged surfaces containing TMA-DPH. The surface charge density of TMA-DPH self-organized structures is expected to be higher than that of PC:TMA-DPH mixed bilayer vesicles.

3.4. Fluorescence anisotropy

Fig. 4 shows the effect of ONP on fluorescence anisotropies of DPH and TMA-DPH in liquid crystalline (EPC) as well as in gel phases (dpPC). In EPC (Fig. 4a), the DPH fluorescence anisotropy ($A_{DPH} = 0.125$) was lower than that of TMA-DPH ($A_{TMA\text{-}DPH} = 0.208$) in the absence of ONP. Up on increasing the ONP concentration, anisotropy values of both probes followed a non-linear behavior with a downward curvature and a slight increase in $A_{TMA\text{-}DPH}$ was observed at [ONP] < 1 mM (Fig. 4a).

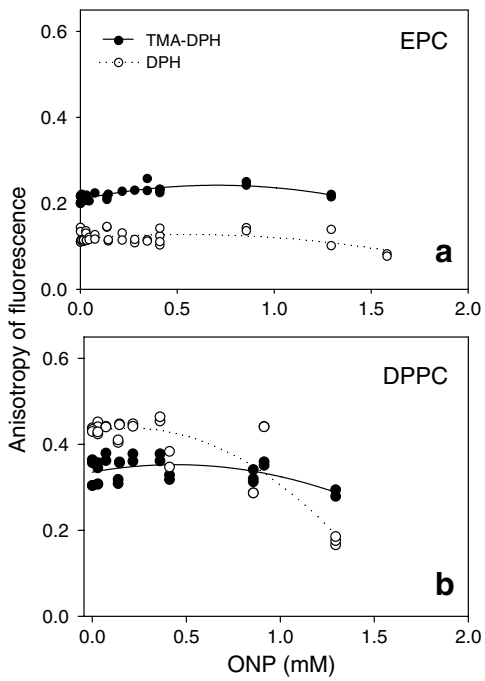

Fig. 4. Effect of ONP on the steady-state fluorescence anisotropy of DPH and TMA-DPH in phospholipids bilayers in fluid (a) and gel (b) phases.

In dpPC control samples, in the absence of ONP, the anisotropy order was $A_{DPH} = 0.434 > A_{TMA\text{-}DPH} = 0.332$. This order was reverted at [ONP] ⩾ 1 mM due to the stronger decrease in A_{DPH} (up to 0.180) if compared with that of $A_{TMA\text{-}DPH}$ (up to 0.286) at [ONP] ⩾ 1.3 (Fig. 4b). Note that in the presence of [ONP] > 1 mM, A_{DPH} values in dpPC reached those measured in EPC, suggesting that ONP induced a gel to liquid crystalline phase transition of dpPC.

4. Discussion

In fluorescence experiments, small (SUVs) or large (LUVs) unilamellar vesicles are usually preferred to be used as model membranes instead of multilamellar vesicles (MLVs) due to the lower diameter of the formers, and consequently to their lower light scattering effect, if compared with the latters. However, to contribute to the understanding of ONP-membrane interaction on the activity of β-Galactosidase it was important to keep the curvature of the lipid–water interface within the same range used previously [9,10] (note that the activity of this enzyme was sensitive to surface curvature). At the same time we tried to keep the light scattering at low levels by the use of a lipid concentration that allowed the fluorescence intensity to remain within linear range in the intensity vs concentration plot (not shown).

DPH and TMA-DPH localize at different depths within bio-membranes [16]. DPH, being highly hydrophobic, partitions within the hydrocarbon chains region of bilayers [19]. On the other hand, TMA-DPH bears a net positive charge in its ammonium moiety that turns the molecule hydrophilic, becoming trapped with its DPH moiety at the polar head group region of membrane bilayers [13]. We studied the ability of ONP to quench the fluorescence emitted by DPH and TMA-DPH assuming that a differential effect would reveal its localization at different depths within the membrane.

A fraction of molecules in the excited state are instantaneously deactivated just after their formation when the quencher is randomly positioned in the proximity of the fluorescent molecule during its excitation and the quencher interacts very strongly with the fluorophore. Hence the sphere of action "v" represents the active volume element

surrounding the fluorophore in its excited state. Instantaneous quenching occurs in a randomly distributed system when a quencher happens to reside within a volume v having a radius r, also called as kinetic distance [16]. It has been shown that quenching occurs when the kinetic distance is bigger than the sum of the radii of solute and quencher [22]. If we take into account that DPH and TMA-DPH loose degrees of freedom up on partitioning in MLVs and that TMA-DPH in water may be self-aggregated into micelles [13], it can be concluded that the DPH-ONP system in water is the only condition tested in the present work that can be considered as random at the molecular level. Moreover, the radii of DPH and TMA-DPH in MLVs as well as TMA-DPH in water should be considered as equivalent to the radii of the self-organized structures where the fluorophores are contained and hence, much larger than the molecular radius of DPH. The higher randomness and the shorter radii of DPH monomers, may explain the fact that, in solution, this probe exhibited the longest kinetic distance and that its half maximal quenching was reached at the lowest concentrations of ONP. When lifetimes of the excited states were considered, DPH in solution exhibited a higher intrinsic probability to be quenched by ONP than DPH in the membrane ($K_{q,DPH,water} > K_{q,DPH,MLVs}$). Interestingly, the intrinsic quenching efficiency of ONP in MLVs was lower for DPH than for TMA-DPH ($K_{q,DPH,MLVs} < K_{q,TMA\text{-}DPH,MLVs}$) which confirmed the low accessibility of ONP to the deeper, and more hydrophobic, regions of the bilayer which are characterized by a low dielectric constant, e.g., $D \cong 4$ [23]. This was also demonstrated through ONP acid–base equilibrium experiments (not shown).

Anisotropy data gave a complementary information about interactions between ONP and the lipid components of the bilayers and the effect its presence had in the motion of phospholipid molecules that is related to the microviscosity of bilayers.

In the liquid crystalline bilayers of EPC, the highest molecular order was evidenced at the polar head group region as sensed with TMA-DPH (Fig. 4a). A generalized slight disordering effect of ONP on the already disordered fluid phase was observed at the highest concentrations tested. (Fig. 4a). In gel phase dpPC bilayers the hydrocarbon chain region resulted the molecular environment that imposed the highest constraints to changes in the probe's order and mobility (Fig. 4b) and it was also the region that suffered the strongest order-disrupting effect of ONP. The results obtained in the absence of ONP were all in accordance with previously reported data [20] while those obtained in its presence strongly suggested the occurrence of a gel to liquid crystalline phase transition of dpPC at [ONP] > 1 mM. The slight increase in $A_{TMA\text{-}DPH}$ observed in the EPC bilayer in the fluid phase at [ONP] < 1 mM (Fig. 4a) might be indicating a rigidifying effect of ONP at the lipid–water interface by increasing the strength of intermolecular interactions at the polar head groups. It is important to note that within the experimental conditions applied to the quenching experiments in the present work (fluid phase bilayers and [ONP] ⩽ 0.8 mM) the order state of the membrane remained approximately constant.

The differential ability of ONP to quench two types of fluorescent probes with different localization within the lipid bilayer suggested that ONP, a weak hydrophobic substance, concentrated in the membrane with respect to the aqueous phase through stabilization forces, which are related with dipolar interactions between ONP and the polar head groups of the membrane components. This localization, which should be thought as a maximum in the ONP concentration profile across the membrane thickness, may play significant roles in the modulation of the hydrolytic mechanism of reactions where this compound is obtained as a product [12]. Moreover, modulation of membrane bound proteins may be achieved through modifications of general membrane properties induced by ONP, such as local surface curvature [24,25].

Acknowledgements

The present work was partially financed by grants from CONICET, SECyT-Universidad Nacional de Córdoba and ANPCyT. J.M.S. and A. del V.T. are fellowship holders and M.A.P. is a Career Investigator from CONICET.

References

[1] R.P. Schwarzenbach, R. Stierli, B.R. Folsom, J. Zeyer, Compounds properties relevant for assessing the environmental partitioning of nitrophenols, Environ. Sci. Technol. 22 (1989) 83–92.
[2] J. Zeyer, H.P. Kocher, Purification and characterization of a bacterial nitrophenol oxygenase which converts *ortho*-nitrophenol to catechol and nitrite, J. Bacteriol. 170 (1988) 1789–1794.
[3] J. Sikkema, J.A.M. Bont, B. Poolman, Interaction of cyclic hydrocarbons with biological membranes, J. Biol. Chem. 269 (1994) 8022–8028.
[4] O.P. Hamill, B. Martinac, Molecular basis of mechanotransduction in living cells, Physiol. Rev. 81 (2001) 685–740.
[5] M.A. Perillo, D.A. García, Flunitrazepam induces geometrical changes at the lipid–water interface, Colloids Surf. 20 (2001) 63–72.
[6] D.A. García, S. Quiroga, M.A. Perillo, Flunitrazepam partitioning into natural membranes increases the surface curvature and alters the cellular morphology, Chem. Biol. Int. 129 (2000) 263–277.
[7] L.M.A. Pinto, S.V.P. Malheiros, E. de Paula, M.A. Perillo, Hydroxyzine, promethazine and thioridazine interaction with phospholipid monomolecular layers at the air–water interface, Biophys. Chem. 119 (2006) 247–255.
[8] R. Lipowski, Domains and rafts in membranes – hidden dimensions of self-organization, J. Biol. Phys. 28 (2002) 195–210.
[9] J.M. Sanchez, M.A. Perillo, Membrane adsorption or penetration differentially modulates β-galactosidase activity against soluble substrates, Colloids Surf. B 24 (2002) 21–31.
[10] J.M. Sanchez, M.A. Perillo, Membrane topology modulates β-galactosidase activity against soluble substrates, Biophys. Chem. 99 (2002) 281–295.
[11] M.H. Abraham, C.M. Du, J.A. Platts, Lipophilicity of the nitrophenols, J. Org. Chem. 65 (2000) 7114–7118.
[12] J.M. Sanchez, I. Ciklic, M.A. Perillo, Effect of partitioning equilibria on the activity of β-galactosidase in heterogeneous media, Biophys. Chem. 118 (2005) 69–77.

[13] F.G. Prendergast, R.P. Haugland, P.J. Callahan, 1-[4-(Trimethylamino)-6-phenylhexa-1,3,5-triene: synthesis, fluorescence properties, and use as a fluorescence probe of lipid bilayers, Biochemistry 20 (1981) 7333–7338.
[14] A.D. Bangham, M.W. Hill, N.G.A. Miller, in: E.D. Korn (Ed.), Methods in Membrane Biology, Plenum Press, New York, 1974, pp. 1–68.
[15] R. Koynova, M. Caffey, Phases and phase transitions of the phosphatidylcholines, Biochim. Biophys. Acta 1376 (1998) 91–145.
[16] J.R. Lakowics, in: Principles of Fluorescence Spectroscopy, Plenum Press, New York, 1986.
[17] R.R. Sokal, F.J. Rohlf, Introduction to Biostatics, Freeman, San Francisco, CA, 1980.
[18] Z.J. Huang, R.P. Hauglnand, Partition coefficients of fluorescent probes with phospholipids membranes, Biochem. Biophys. Res. Commun. 181 (1991) 166–171.
[19] B.R. Lentz, S.W. Burgess, A dimerization model for the concentration dependent photophysical properties of diphenylhexatriene and its phospholipids derivatives DPHpPC and DPH pPA, Biophys. J. 56 (1989) 723–733.
[20] G. Duportail, A. Weinreb, Photochemical changes of fluorescent probes in membranes and their effect on the observed fluorescence anisotropy values, Biochim. Biophys. Acta 739 (1983) 171–177.
[21] A.S. Ira, R. Koti, G. Krishnamoorthy, N. Periasamy, TRANES spectra of fluorescence probes in lipid bilayer membranes: an assessment of population heterogeneity and dynamics, J. Fluoresc. 13 (2003) 95–103.
[22] R. Guiri, Fluorescence quenching of coumarins by halide ions, Strochim. Acta A 60 (2004) 757–763.
[23] A. Alonso, R. Sáez, F.M. Goñi, The interaction of detergents with phospholipid vesicles: a spectrofluorimetric study, FEBS Lett. 137 (1982) 141–145.
[24] A. Seelig, P. Allegrini, J. Seelig, Partitioning of local anesthetics into membranes: surface charge effects monitored by the phospholipid head-group, Biochim. Biophys. Acta 939 (1988) 267–276.
[25] M.A. Perillo, D.A. García, Flunitrazepam induces geometrical changes at the lipid–water interface, Colloids Surf. 20 (2001) 63–72.